

The crustal nature of the northern Mozambique Ridge, Southwest Indian Ocean

Nelta David Matsinhe^{1, 2}, Yong Tang^{1, 2, 3, 4, 5, 6*}, Chun-Feng Li^{1, 7}, Jiabiao Li²,
Estevão Stefane Mahanjane⁸, He Li^{1, 2}, Yinxia Fang²

¹Institute of Marine Geology and Resources, Zhejiang University, Zhoushan 316021, China

²Key Laboratory of Submarine Geosciences, Second Institute of Oceanography, Ministry of Natural Resources, Hangzhou 310012, China

³School of Oceanography, Shanghai Jiao Tong University, Shanghai 200240, China

⁴Southern Marine Science and Engineering Guangdong Laboratory (Zhuhai), Zhuhai 519080, China

⁵College of Marine Science and Technology, China University of Geosciences, Wuhan 430074, China

⁶College of Marine Geosciences, Ocean University of China, Qingdao 266100, China

⁷Laboratory for Marine Mineral Resources, Pilot National Laboratory for Marine Science and Technology (Qingdao), Qingdao 266237, China

⁸Institute National Petroleum (INP), Maputo 4724, Mozambique

Received 17 September 2020; accepted 5 November 2020

© Chinese Society for Oceanography and Springer-Verlag GmbH Germany, part of Springer Nature 2021

Abstract

The Mozambique Ridge (MOZR) is one of the basement high structures located in the Southwest Indian Ocean, parallel to the Southeast African continental margin. It was formed as a result of the tectono-magmatic evolution of the Gondwana breakup. The origin of the MOZR has been highly debated, with models suggesting either continental or oceanic origin. With new free-air gravity anomaly and multichannel seismic (MCS) reflection data, we present results of 2D density modeling along two seismic profiles acquired by R/V *Xiangyanghong 10* at the northern Mozambique Ridge (N-MOZR) between 26°S and 28°S. We observed high free-air gravity anomaly and strong positive magnetic anomaly related to the emplaced seaward dipping reflectors (SDR) and high density lower crustal body (HDLCB), and high Bouguer gravity anomaly associated with the thinning of the continental crust underneath the N-MOZR over a distance of ~82 km. This suggests a thinned and intruded continental crust bound by the Mozambique Fracture Zone (MFZ) that is characterized by gravity low and negative magnetic anomaly. This fracture zone marks the continent-ocean boundary (COB) while the N-MOZR is the transform margin high, i.e., marks the continent-ocean transition (COT) of the Southern Mozambique margin, following the definition of transform margins. We suggest that the N-MOZR was formed by continental extension and subsequent breakup of the MFZ, accompanied by massive volcanism during the southward movement of the Antarctica block. The presence of SDR, HDLCB, and relatively thick oceanic crust indicates the volcanic nature of this transform margin.

Key words: crustal nature, northern Mozambique Ridge, seaward dipping reflection, gravity modeling, continent-ocean transition, continent-ocean boundary

Citation: Matsinhe Nelta David, Tang Yong, Li Chun-Feng, Li Jiabiao, Mahanjane Estevão Stefane, Li He, Fang Yinxia. 2021. The crustal nature of the northern Mozambique Ridge, Southwest Indian Ocean. *Acta Oceanologica Sinica*, 40(7): 170–182, doi: 10.1007/s13131-021-1747-9

1 Introduction

The East African Margin is a geotectonic feature with a wide range of geological frameworks that can help us understand the Gondwana breakup processes. The margin was formed due to the opening between Africa and Antarctica during the Jurassic Period. Several studies investigated the tectono-magmatic evolution of the Gondwana Supercontinent and provided a full paleogeographic reconstruction of the supercontinent (Rabinowitz et al., 1983; Coffin and Rabinowitz, 1992; Cox, 1992; Reeves and De Wit, 2000; Jokat et al., 2003; Eagles and König, 2008; König and Jokat, 2010; Reeves et al., 2016; Leinweber and Jokat, 2012; Nguyen et al., 2016; Thompson et al., 2019; Mueller and Jokat, 2018). The breakup of Gondwana is thought to be related to the Karoo

(Bouvet) mantle plume (Cox, 1992; Jokat et al., 2003; Reeves, 2009, 2014; Reeves and Mahanjane, 2013; Reeves et al., 2016), where the basement structure was the main factor controlling the distribution of the Bouvet mantle plume, which flowed in three directions, forming the Mwenezi Triple Junction: the Lebombo, Okavango, and Limpopo-Angoche dyke swarms that formed the Karoo-Ferrar Large Igneous Province prior to the Gondwana Breakup (Riley and Knight, 2001; Eagles and König, 2008; Klausen, 2009; Leinweber and Jokat, 2012; Svensen et al., 2012; Hastie et al., 2014; Reeves et al., 2016). Reeves and Mahanjane (2013) showed that the movement of Eastern Gondwana followed a dextral strike-slip pattern defined by the Davie Fracture Zone (DFZ) and Lebombo-Explora segments in the earliest phase

Foundation item: The National Key R&D Program of China under contract No. 2017YFC1405504; the National Natural Science Foundation of China under contract Nos 41830537, 4176113405 and 41476048.

*Corresponding author, E-mail: tangyong@sio.org.cn

of Gondwana's disruption (183 Ma). The strike-slip setting changed to a transform setting when the seafloor spreading started ca. 155.3 Ma between Africa and Antarctica (König and Jokat, 2010; Hastie et al., 2014).

According to the paleogeographic reconstruction model proposed by Reeves et al. (2016), the initial rift phase of Gondwana was in the NE-SW direction parallel to the Limpopo-Angoche dyke swarm during 188 Ma to 170 Ma, similar to the Karoo rift geometry in Africa (300 Ma to 200 Ma) (De Wit, 2003). This model suggests that the initial phase of the breakup of Gondwana in the Middle to Late Jurassic was a result of the reactivation of the Karoo tectonic event, and considered three rifting episodes in Africa: The Karoo (300 Ma to 200 Ma), Early Jurassic-Aptian (183 Ma to 120 Ma) and East African Rift (25 Ma to 0 Ma). Klimke et al. (2018) proposed that Antarctica initially moved away from Africa in a WNW-ESE direction between 184 Ma and 171 Ma and then changed the direction to SSE, whereas Nguyen et al. (2016) suggested an NNW-SSE opening. These different interpretations, according to Mueller and Jokat (2018), result from the lack of high quality geophysical data along the conjugate margins of the Africa-Antarctica corridor (AAC), leading to several problems constraining the early plate movement during the Gondwana opening.

The subsequent southward drift of Antarctica relative to the African block formed the Mozambique basin off the coast of Africa and the Riiser-Larsen Sea, north of the conjugate Antarctica margin between the DFZ in the east and the Mozambique Fracture Zone (MFZ) in the west, along the AAC (Senkans et al., 2019).

Studies based on paleogeographic reconstruction models and seismic data (reflection and refraction) interpretation indicate that the Gondwana breakup had two main stages of rifting in the south, which supports a rift jump model (Cox, 1992; Mahanjane, 2012; Mueller et al., 2016). Breakup stage I relates to the development of the first Karoo rift that ended along the northern Zambezi Coast with the emplacement of the Angoche dykes, around 170 Ma (Reeves and De Wit, 2000); this was post-rift magmatism as a result of the reactivation of the Pebane shear zone. Breakup stage II relates to the development of rift II located along the southeastern edge of the Beira High (Mahanjane, 2012). This rift was mostly magma-poor, but with strong distensive deformation, giving rise to the final breakup of Gondwana and the onset of oceanic crust during 166 Ma to 154 Ma based on magnetic anomaly data (Jokat et al., 2003; König and Jokat, 2010; Senkans et al., 2019). Most of the paleogeographic reconstruction models converge to approximately (183±1) Ma and provide new insights into the Gondwana breakup and the onset of oceanic crust. However, the consensus concern this matter is far from being achieved, regarding the initial position of Antarctica block at the time of the breakup, with one hypothesis defending a loose fit between Africa and Antarctica block and another hypothesis suggested by recent studies, defending a tighter fit implying a large overlap of the blocks, presuming oceanic origin for the Mozambique Coastal Plain (MCP), northern Natal Valley (NNV) and Mozambique Ridge (MOZR) (Eagles and König, 2008; Leinweber and Jokat, 2012; Mueller and Jokat, 2018). Therefore, some issues remain unclear, such as the nature of the crust in the MOZR, and the demarcation of the continent-ocean Transition (COT) and the continent-ocean boundary (COB) in the southern Mozambique margin.

In this study, we divided the MOZR into the northern, central, and southern regions, following previous studies (Hanyu et al., 2017; Fischer et al., 2017) (Fig. 1). Based on new gravity and seismic reflection data surveyed by R/V *Xiangyanghong 10* on the northern Mozambique Ridge (N-MOZR) and Mozambique Basin

(MB), we discuss the crustal nature of the N-MOZR and the continent-ocean transition (COT) of the southern Mozambique margin and provide new information on Gondwana reconstructions.

2 Definition and demarcation of the COT and COB

The continent-ocean transition represents the zone that archives the complex mechanisms from continental rifting to the onset of seafloor spreading. Therefore, the identification and understanding of the COT can provide valuable information concerning the geological processes related to the continental breakup. The classification of the COT is usually based on melt supply (Eagles et al., 2015). Therefore, Whitmarsh and Miles (1995) proposed three main interpretations for the formation of the COT based on the above classification: (1) heavily intruded and extended continental crust; (2) exhumed upper mantle material; and (3) ultraslow seafloor spreading. The COT along the magma-rich or volcanic margin is defined as a zone of highly intruded and stretched continental crust with igneous rocks in the form of seaward dipping reflectors (SDR), and high velocity lower crust beneath the stretched continental crust (Mjelde et al., 2007; Minshull, 2009; Blaich, 2013). For the magma-poor rifted margins, the COT is usually expressed in the form of hyper-extended continental crust, with limited or absent of syn-rift magmatism, serpentinized peridotites, detachment fault, rotated fault blocks with seaward dipping faults (Sutra et al., 2013; Gao et al., 2015). In this type of margins, the COT is considerably wider compared to magma-rich and transform margins. Furthermore, for the transform margins, the COT is usually described as abrupt compared to the rifted margins, comprising marginal ridge rising 1–3 km above the seafloor, and the seaward termination of the COT is characterized by a transform fault separating continental crust from the oceanic crust (Lorenzo and Wessel, 1997; Bird, 2001; Berndt et al., 2001). The identification of COT in the passive margins is strictly associated with magmatism (SDR, HVLCB, volcanoes), crustal thickness changes, changes in the Moho depth, typical gravity, and magnetic signatures.

Several studies attempted to mark the COT and COB along the Mozambique continental margin, where most of them focused on the central part of the margin. Leinweber et al. (2013), using P-wave and 2D density models, observed typical characteristics of the magma-rich margins, with SDR, stretched continental crust and magmatic underplating on the COT, also corroborated by Mueller et al. (2016) and Nguyen et al. (2016) that placed the COB close to the coast. In our study area, some authors tried to demarcate the COT and COB based on the understanding of the MOZR nature. The correct name is Darracott (1974), based on gravity and isostatic data, suggested that the Mozambique coastal plain (MCP), northern Natal Valley (NNV), and MOZR were the transitional crust of the southern Mozambique margin, supported by Mahanjane (2014). While Leinweber and Jokat (2011) proposed that part of the MCP and NNV were the COT, but the entire MOZR was purely from oceanic origin, on the other hand, Hanyu et al. (2017) suggested that the N-MOZR and central Mozambique Ridge (C-MOZR) were part of the COT, placing the COB between C-MOZR and southern Mozambique Ridge (S-MOZR).

3 Geological setting

The MOZR is a large N-S trending structure lying roughly parallel to the southeast coast of Africa between 25°S and 35°S. It is bordered in the east by the 5 000-m deep Mozambique Basin and west by the Natal Valley, which separates this ridge from the Southeastern African continental margin. As one of the many

aseismic structures located in the SW Indian Ocean, the nature of the MOZR, whether continental or oceanic, is still under debate. Several geophysical and geological studies proposed that the entire ridge is underlain by either continental crust (Dingle et al., 1978; Lyakhovskiy et al., 1994; Marks and Tikku, 2001; Tikku et al., 2002; Eagles and König, 2008), transitional crust (Darracott, 1974; Martin and Hartnady, 1986; Mahanjane, 2014), or oceanic crust (Maia et al., 1990; Green, 1972; König and Jokat, 2010; Leinweber and Jokat, 2011; Gohl et al., 2011). Other researchers divided the ridge into the northern and central Mozambique Ridge of continental origin, and the southern Mozambique Ridge of oceanic origin (Hanyu et al., 2017; Fischer et al., 2017).

The basement rock of the C-MOZR was sampled from the Deep Sea Drilling Project (DSDP) Site 249, where tholeiitic basalt was observed with a composition similar to weathered mid-ocean ridge basalt. DSDP Site 248 in the Mozambique Basin, 150 km east of DSDP Site 249, recovered basalts distinct from the average MORB-like rocks that, according to Simpson (1974), fall within the range of Karoo basalts from Lebombo Monocline (Fig. 1c). Nevertheless, dredged rock samples DR1 and DR3 collected on R/V *Marion Dufresne*-MD60-MACAMO (Mougenot et al., 1991), and DRQ collected on R/V *Professor Logachev* (Ben-Avraham et al., 1995) support a continental affinity for the southern and central MOZR. The DRQ rock samples are similar to rocks found in Namaqua Province of Southern Africa, implying that part of the southern MOZR was a microcontinental fragment embedded into oceanic crust, associated with a zone of contemporary lithospheric stretching (Ben-Avraham et al., 1995).

Recent studies using high-resolution magnetic potential field data suggested that the entire MOZR was an indication of a long-lasting interaction between a mantle plume and the Antarctic plate boundary during the opening between Africa and Antarctica from 140 Ma to 122 Ma (König and Jokat, 2010; Leinweber and Jokat, 2011). Deep crustal ocean bottom seismometer data and multichannel seismic reflection data provided evidence that the southern MOZR is predominantly of oceanic origin, and probably formed due to excessive volcanism and magmatic accretion phases (Gohl et al., 2011; Fischer et al., 2017). For the central and southern MOZR, the geophysical data indicate a large igneous province (LIP).

However, little is known about the N-MOZR. The magnetic anomaly study done by Leinweber and Jokat (2011) concluded that the N-MOZR was formed by large-scale volcanism, while Hanyu et al. (2017), Thompson (2017), and Moulin et al. (2019) suggested a stretched continental crust, using vector geomagnetic anomaly and satellite gravity data, and wide-angle seismic data, respectively. The nature of the MOZR is one of the critical points for the demarcation of the COT and COB along the southern Mozambique margin.

4 Data acquisition and processing

4.1 Multichannel seismic data

The seismic reflection survey was conducted in June 2016 during the China-Mozambique Joint Cruise onboard the R/V *Xiangyanghong 10*. This survey was performed under the cooperation between Second Institute of Oceanography, State Oceanic Administration, China) and the IMAF (Boundaries and Maritime Institute, Mozambique), from June 1 to 23, 2016. During the cruise, geophysical data were acquired along the southern Mozambique Margin (Fig. 1). The seismic01 profile is 359 km long, lying NW–SE from the northern Natal Valley, across the

northern Mozambique Ridge, into the Mozambique Basin. The seismic02 profile is 351 km long, lying W–E from the Northern Mozambique Ridge into the Mozambique Basin. A total of 710 km of 2D high-resolution multichannel seismic profiles were recorded using a 108-channel streamer (active length of 1 475 m) with an interval spacing of 12.5 m. The source consisted of four G-gun airgun arrays with a total volume of 1 340 cubic inches (1 cubic inch=0.016 387 037 037 L), working pressure of 13 790 kPa, towed at 10 m depth, at a shot interval of 50 m. The recording length was 14 s two-way travel time (TWT), and the sampling rate was set at 2 ms.

Overall, the quality of reflection seismic data is good. The standard seismic processing of the data was provided by China National Offshore Oil Corporation, which involved the comprehensive treatment (including stack, migration, and velocity analysis). The processing flow included: de-noising, amplitude compensation, energy equalization of gun offset, surface-related multiple elimination, diffracted multiple attenuation, de bubble using predictive de-convolution, common reflection surface stacking, pre-stack isotropic ray-traced Kirchhoff time migration (PSTM,) and pre-stack depth migration (PSDM). During the PSTM, a precise velocity analysis was carried out, and the stacking velocities were converted into interval velocities and set up to the velocity field for the migration process, and then we did the time-depth conversion. The data were processed using CGG GEOCLUSTER 5000, Westerngeco Omega 2.0, Paradigm EPOS3/4 software, and then was loaded to the GeoFrame/IESX software for further data interpretation.

4.2 Gravity and magnetic data

The free-air gravity anomaly data were collected along nine profiles with a total length of 4 500 km by R/V *Xiangyanghong 10*, using the Air-Sea Gravity System II Marine Gravimetry System (S-129) produced by LaCoste and Romberg, USA. The gravity data were processed following the traditional marine gravity data processing flow, described in more detail by Wang et al. (2018). We used these data to perform 2D gravity modeling along the multichannel seismic (MCS) reflection data (seismic01 and seismic02) to determine the nature of the crust in the N-MOZR. The Bouguer gravity anomaly data were obtained from the world gravity model (WGM 2012) (Bonvalot et al., 2012). The WGM2012 model was derived from earth global gravity models EGM2008 and DTU10 with 1'×1' resolution terrain corrections derived from ETOPO1. The total field magnetic anomaly data were derived from the global earth magnetic anomaly grid (EMAG2) (Maus et al., 2009). The EMAG2 dataset was compiled from satellite, airborne, and marine magnetic measurements at 4 km altitude above the geoid with 2-arcmin resolution.

4.3 Gravity modeling

Gravity modeling was carried out using the interactive gravity and magnetic modeling program GM-SYS (from the northwest Geophysical Associates, Inc.). The aim of the gravity modeling was to achieve a consistent geological model that corresponds to the geology of the study area. The modeling was performed by continuously apply small adjustments to the geometries and density values until a good match between observed and calculated gravity anomalies was achieved, which fell within the acceptable error for this method of no more than 10×10^{-5} cm/s² (Ljones et al., 2004; Antobreh et al., 2009)

As the first step, a depth-converted seismic data was incorporated to get the starting depth model. The following step was to

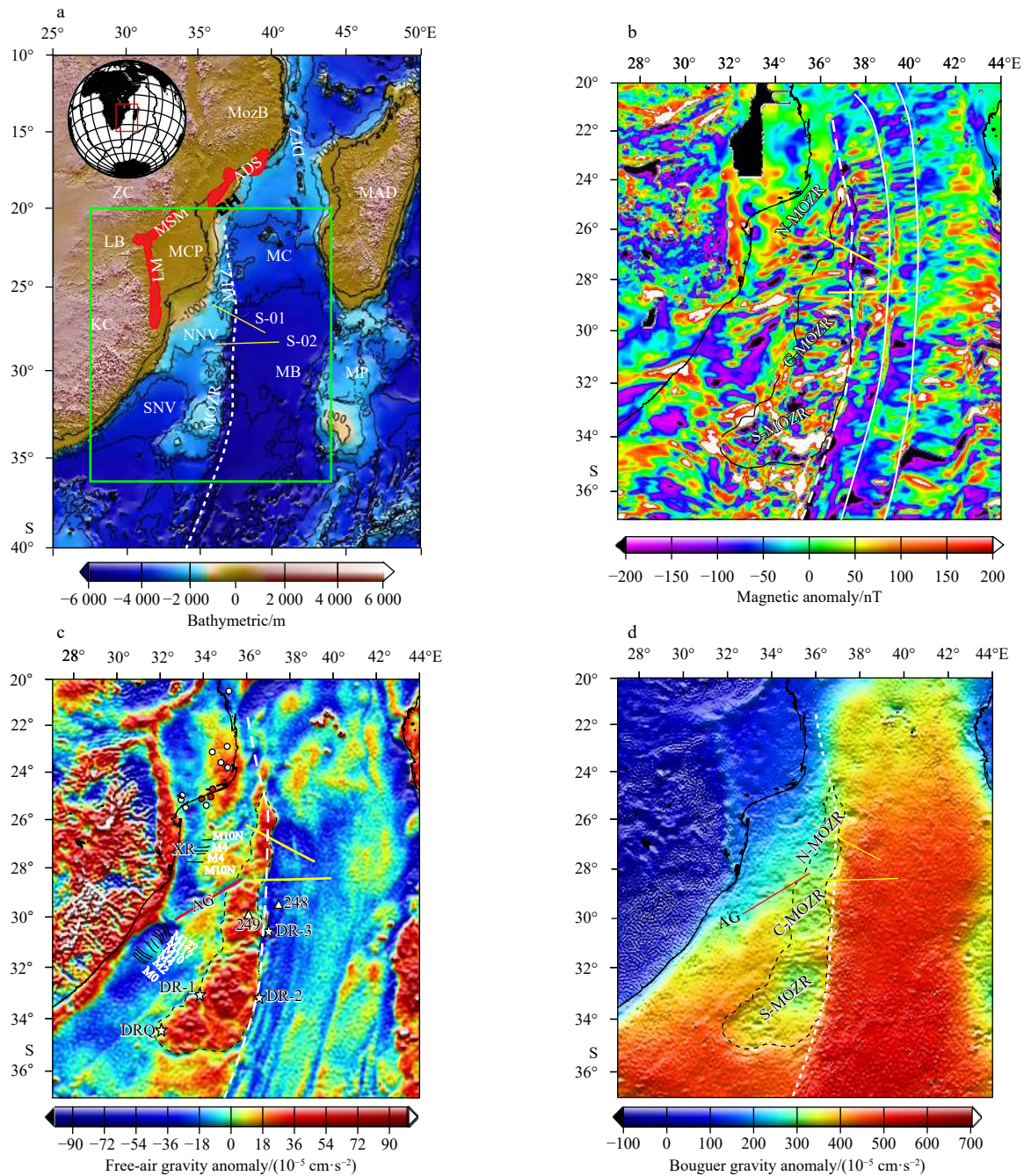


Fig. 1. Tectonic overview of the Mozambique passive margin and Mozambique Ridge (MOZR). a. Bathymetric map (data from GEBCO_2014, https://www.gebco.net/data_and_products/gridded_bathymetry_data/), with 1 000-m contours in black, showing the dominant geological features and magnetic anomalies. In a, the solid yellow lines along the northern MOZR (N-MOZR) mark the location of our seismic and gravity profiles. b. Magnetic anomaly (data from EMAG2, <http://geomag.org/models/emag2.html>). In b, the black lines indicate the fracture zones along the Mozambique Basin, with one of them crossing the N-MOZR. c. Free-air gravity anomaly map (data from WGM2012, <http://bgi.omp.obs-mip.fr/data-products/Grids-and-models/wgm2012>). In c, the NW–SE black lines indicate the magnetic anomalies M12 to M0 identified by Goodlad et al. (1982); the W–E black lines indicate the magnetic anomalies M10N and M4, and XR is the extinct spreading center proposed by Marks and Tikku, 2001; the white triangles are Deep Sea Drilling Project (DSDP) Sites 248 and 249 (Simpson, 1974); the white stars are the rock samples DR1, DR2, DR3, DRQ (Ben-Avraham et al., 1995; Mougnot et al., 1991); the white circles in c are wells located along the Mozambique Coastal Plain; the three red circles show the wells that recovered the Early Cretaceous basalts; and the solid red line refers to the Ariel Graben (AG). d. Bouguer gravity anomaly map (data from WGM2012, <http://bgi.omp.obs-mip.fr/data-products/Grids-and-models/wgm2012>). S-01: Seismic01; S-02: Seismic02; MozB: Mozambique Mobile Belt; ZC: Zimbabwe Craton; LB: Limpopo Belt; KC: Kaapval Craton; MCP: Mozambique coastal plain; MC: Mozambique Channel; DFZ: Davie Fracture Zone; NNV and SNV: Northern and Southern Natal Valley; MFZ: Mozambique Fracture Zone; MOZR: Mozambique Ridge; N-MOZR: northern Mozambique Ridge; C-MOZR: central Mozambique Ridge; S-MOZR: southern Mozambique Ridge; MB: Mozambique Basin; MP: Madagascar Plateau; MAD: Madagascar.

develop a simple 4-layer crustal model that included the seawater, sediments, crust (continental and oceanic), and mantle. To obtain the initial geometries for these four layers, we based on the interpretation of the most prominent reflectors from the seismic reflection data. The seismic profiles were depth-converted using velocity functions obtained from interval velocities based on stacking velocities from MCS data. The assigned densities were based on previous studies done in the Mozambique margin and well known rifted volcanic margins (e.g., Mjelde et al., 2005; Hirsch et al., 2007; Voss and Jokat, 2007; Leinweber et al., 2013; Müller, 2017).

5 Results

The modeled density with the calculated and observed gravity data for the profiles seismic01 and seismic02 are shown in Figs 3 and 4. The Moho depth for these profiles along the Mozambique Ridge was mainly inferred from the gravity anomaly data because no corresponding seismic reflectors were observed. Overall, there is a good fit between the observed and calculated gravity anomaly, in both models with an absolute error of 1.937×10^{-5} cm/s² for profile seismic01 and 1.143×10^{-5} cm/s² for profile seismic02.

5.1 Profile seismic01

Profile seismic01 is oriented NW-SE and is 354 km long (Fig. 2). We have identified two regional seismic reflectors in the sedimentary basement, the top basalt associated with basalt intrusions (CDP 1–18501) and the oceanic crust (CDP 18501–56204). The interpreted sedimentary sequences followed Gao et al. (2020), which described the stratigraphic framework in detail in the study area. Distinct reflectors typical of volcanic margins, commonly known as seaward dipping reflectors (SDR), can be seen along the N-MOZR between CDP 7401–14801, with ~ 45 km wide. The reflectors show a high-amplitude, a divergent arcuate with dip steepening from sub-horizontal and laterally continuous at little over 4 km depth, and can be observed to at least 5.5 km below the basement. It is also characterized by abrupt strata termination in landward direction, along the basement high (Fig. 3).

No clear observation of fault controlling the SDR unit accommodation was identified. Moreover, toward the MB, we also observed other high-amplitude reflectors between CDP 18501–22201 (Fig. 6a). Below the SDR, we clearly see the transition from low-amplitude reflectors from the N-MOZR to high-amplitude and chaotic reflectors in the Mozambique Basin, separated by deformed reflectors aligned vertically between 7 km and 14 km depth below the basement in the CDP 18501 corresponding to MFZ (Fig. 4). The high amplitude reflectors observed between CDP 18501–22201 appear to accommodate along the fracture zone. The base of the crust in some parts of the MB that we were able to identify is marked by a continuous reflection below 9 s TWT interpreted as Moho discontinuity. From the Moho reflection, we observed that the crust thins to the southeast, from the N-MOZR, where the Moho discontinuity is deeper to MB, where the Moho reflection depth decreases along the major fault deformation in the CDP 40701 (Fig. 5).

The free-air gravity anomaly varies considerably along the profile. The eastern part of the NNV (between 0 km and 50 km) is composed by relatively thinner crust compared to the western part and MCP with 30–35 km (Domingues et al., 2016; Moulin et al., 2019). The free-air anomaly shows a maximum of -80×10^{-5} cm/s², with a positive Bouguer anomaly (less than 300×10^{-5} cm/s²) and magnetic anomaly. At 30–50 km, we observed a gravity low that coincides with a sharp change in crustal thickness. The Moho relief in this area gradually rises from 24 km in the NNV to 14 km in the N-MOZR.

At 50–132 km (across the MOZR), the free-air anomaly shows a maximum peak of -120×10^{-5} cm/s² with a positive Bouguer anomaly (300×10^{-5} – 350×10^{-5} cm/s²) and a local minimum and maximum of -200 nT and 200 nT, respectively, in response of magmatic intrusions (Fig. 3b). At 119–144 km (N-MOZR and MB boundary), the free-air and magnetic anomaly rapidly drop to less than 40 mGal and less than -100 nT, respectively, along the MFZ. Furthermore, the Moho shows a flat topography in this area, until 240–270 km, where the Moho relief very sharply rises to -5 km (Fig. 6c). The free-air anomaly has two local peaks (180–210 km and 240–270 km) due to intrusions and a major

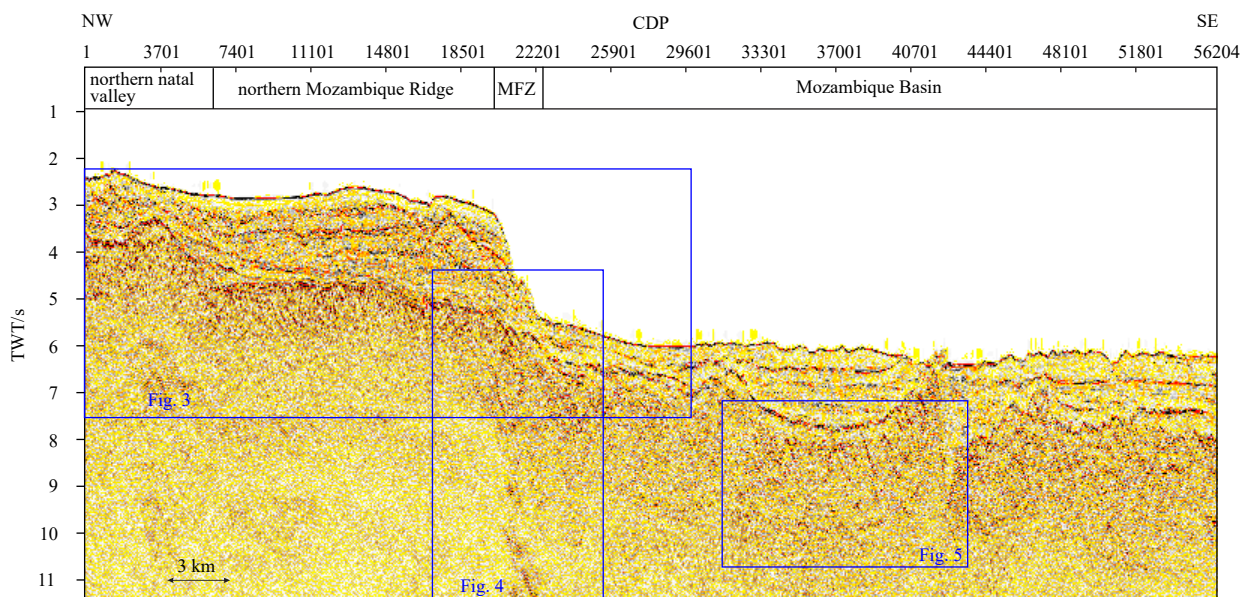


Fig. 2. Uninterpreted seismic01 profile from NW-SE, showing the northern Natal Valley, northern Mozambique Ridge, Mozambique Fracture Zone (MFZ) and Mozambique Basin. TWT: two-way travel time.

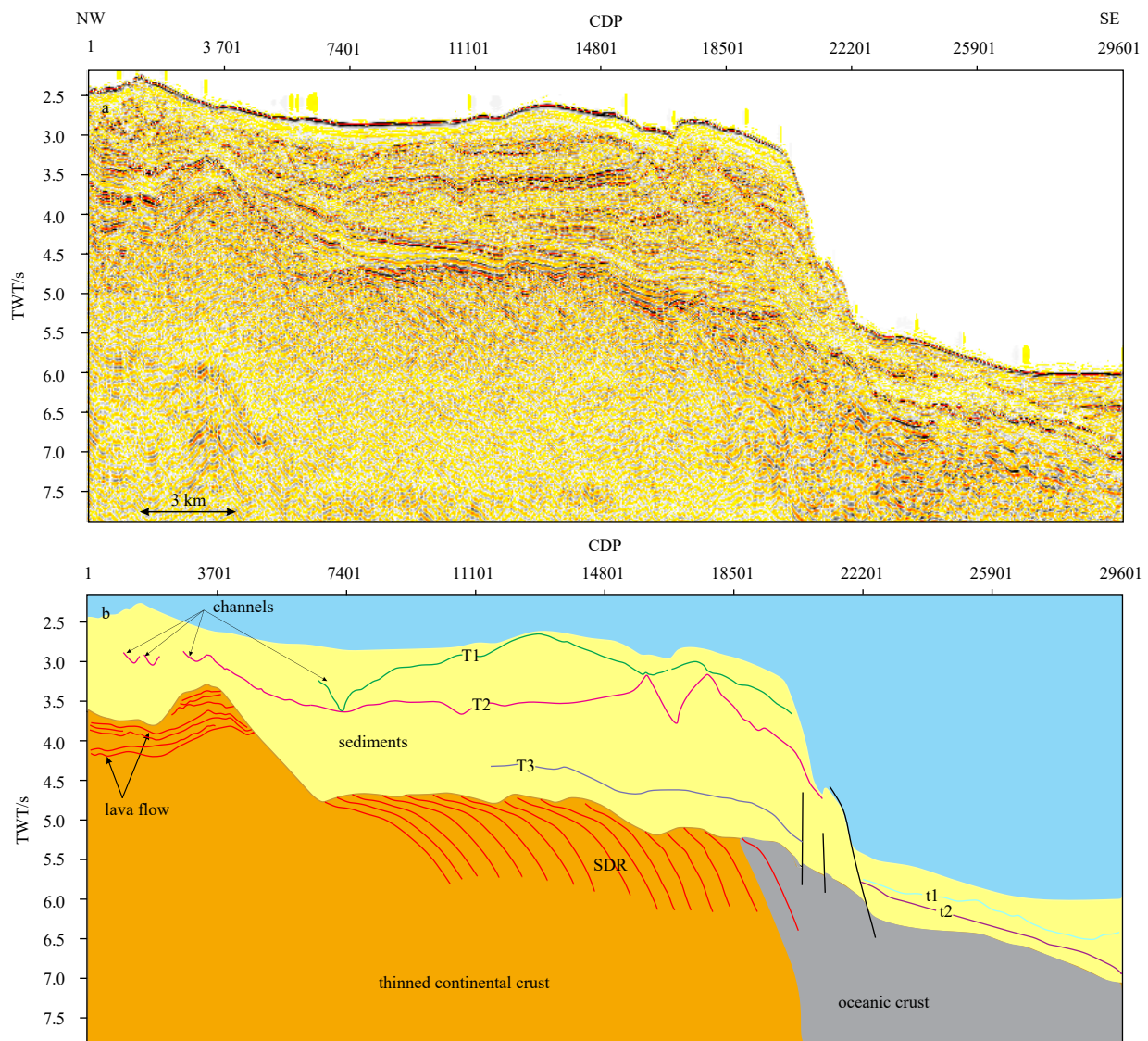


Fig. 3. Enlarged section of profile seismic01 showing the high-amplitude SDR in the northern Mozambique Rudge (N-MOER) (a) and its simple seismic interpretation (b). T1, T2 and T3 are stratigraphic unconformities observed in the N-MOZR, and t1 and t2 are unconformities observed in the Mozambique Basin (Gao et al., 2020). TWT: two-way travel time.

fault, with a negative magnetic anomaly and very high Bouguer anomaly (400×10^{-5} – 450×10^{-5} cm/s²). The oceanic crust in the MB has a thickness of ~9.5 km, which is thicker than normal oceanic crust.

The final density model (Fig. 6d) consists of five layers with densities ranging from 1.03 g/cm³ to 3.33 g/cm³. The water and sedimentary layers have densities of 1.03 g/cm³ and 2.1 g/cm³, respectively. The NNV and N-MOZR crust has a density of 2.87 g/cm³, and the MB crust has a density of 2.9 g/cm³. The mantle was modeled with a density of 3.33 g/cm³. In conformity with wide-angle data (e.g., Moulin et al., 2019), a high density lower crustal body (HDLCB) with 3.19 g/cm³ was added at 0–80 km.

5.2 Profile seismic02

Profile seismic02 is 346 km long with a W-E orientation (Fig. 1b). It is located on the eastern tip of the N-MOZR.

In this seismic profile, we also observed two regional continuous, prominent, high-amplitude reflectors in the sedimentary basement, corresponding to top basalts between CDP 56372 and 48972 in the N-MOZR and the oceanic crust between CDP

48972–8721 (Fig. 7a).

The free-air gravity anomaly along the profile varies between 31×10^{-5} cm/s² and 95×10^{-5} cm/s² (Fig. 7c). Over the N-MOZR between 0 km to 30 km, the gravity anomaly reaches 80–89 cm/s, the magnetic anomaly is constant at 50 nT, and the Bouguer anomaly is positive (320×10^{-5} cm/s²) (Fig. 7b). However, from 30 km to 65 km, we observed a rapid decrease in free-air anomaly near the N-MOZR and MB boundary, along the MFZ to $\sim 40 \times 10^{-5}$ cm/s² that then rises to ~ 60 – 70×10^{-5} cm/s², and remained constant throughout the MB (between 110 km and 340 km). These observations coincide with the changes in the Moho depth, where gradually rises from ~15 km depth in the N-MOZR to 10 km depth in the MB. The magnetic anomaly in the MB fluctuates from negative to positive throughout the basin (–50 nT to 50 nT), with a high positive Bouguer anomaly. The oceanic crust in the MB has a thickness of ~8.1 km, which is thicker than normal oceanic crust.

The final density model (Fig. 7d) consists of a simple layered model with five anomalous density layers, with densities between

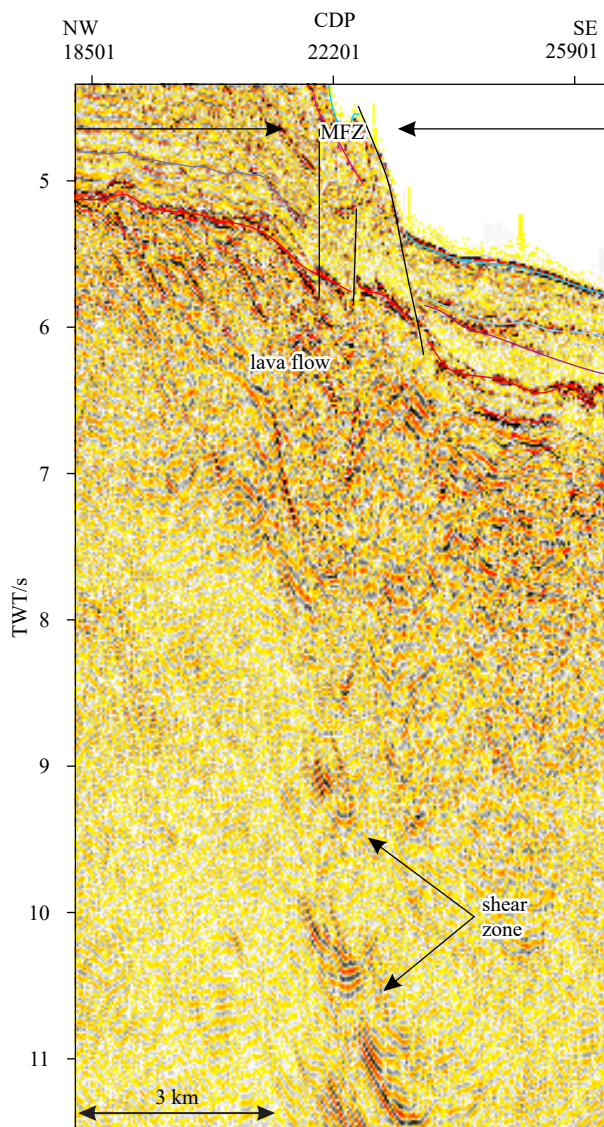


Fig. 4. Seismic profile crossing the Mozambique Fracture Zone, showing the shear zone below the lava flow that separates the low amplitude reflectors from the northern Mozambique Ridge to high amplitude reflectors in the Mozambique Basin. TWT: two-way travel time.

1.03 g/cm³ and 3.33 g/cm³. The water density was set at 1.03 g/cm³, and the sediment density was 2.1 g/cm³. The N-MOZR crust was assigned a density of 2.87 g/cm³, and the MB crust was 2.9 g/cm³. Finally, the mantle was modeled with a density of 3.33 g/cm³.

6 Discussion

6.1 The nature of the northern Mozambique Ridge

Analysis of the seismic reflection data and density models yielded three important results. (1) The N-MOZR is formed by thinned and intruded continental crust, possibly caused by a continental extension, followed by the rupture of the MFZ. (2) The N-MOZR forms the transition zone from typical continental crust to abnormal oceanic crust on the MB, separated by a transform boundary. (3) The presence of SDR, basaltic intrusions, and HDLCB along the N-MOZR suggest that the development of the

transform boundary was accompanied by intense magmatism.

According to Basile (2015), a transform margin is a continent-ocean boundary superposed onto an active or previously active transform fault. Usually, this transform boundary is marked by a high-standing continental marginal ridge, 50–100 km wide, adjacent to a deep sedimentary basin (Lorenzo and Wessel, 1997; Bird, 2001; Berndt et al., 2001); this is consistent with our observations in the N-MOZR. The high-standing marginal ridge may have been induced by thermal uplifting during seafloor spreading (Lorenzo et al., 1991). Moreover, Fischer et al. (2017) and Jacques et al. (2018) showed that the basement high on the MOZR is related to the development of a large igneous province (LIP).

Domingues et al. (2016) observed a seaward thinning of the continental crust from the 35 km thick in the MCP to the 25–30 km thick in the NNV (Moulin et al., 2019), which gradually thinned seaward showed by our results; this is supported by the Bouguer gravity anomaly data (Figs 1d and 6b) showing gravity values above those of the Kaapvaal Craton, implying a shallow Moho depth underneath the N-MOZR. Additionally, the Moho relief in profile seismic01 rises gradually from 24 km depth in the NNV to 14 km depth in the N-MOZR, reflecting a crustal thickness variation from ~18 km in the NNV (Fig. 6: 0–50 km) to ~10 km in the N-MOZR (Fig. 6: 50–132 km and Fig. 7: 0–60 km). Although, our density model has a high depth uncertainty, we believe that it is in agreement with the observations of Domingues et al. (2016) and Moulin et al. (2019). Our models show average densities of 2.87 g/cm³ for the N-MOZR crust, which are in agreement with typical continental crust densities (Christensen and Mooney, 1995) and 2.9 g/cm³ for the MB oceanic crust, and 3.19 g/cm³ for the HDLCB (Figs 6 and 7) (Mjelde et al., 2005; Voss and Jokat, 2007; Leinweber et al., 2013; Müller, 2017).

Several studies have documented the presence of thick wedges of volcanic flows in the rifted margins, commonly associated to volcanic margins that are expressed in seismic data as SDR and HDLCB seaward of the continental rifted margin, between typical continental crust and normal oceanic crust (Korenaga et al., 2000; Menzies et al., 2002; Geoffroy, 2001, 2005; Mjelde et al., 2007; Franke et al., 2013; Leinweber et al., 2013). The high free-air gravity and pronounced positive magnetic anomalies observed along the N-MOZR appear to be related to intrusions in the NNV between 0–40 km (Fig. 6), the deposition of SDR and the HDLCB added between 0–80 km (Figs 3 and 6: 50–132 km; CDP 7401–14801), and basaltic lava flow between 0–52 km observed in seismic reflection data (Fig. 7). The SDR interpreted along the N-MOZR indicate an intense syn-rifting volcanic activity in this ridge (Fig. 1b). Moreover, we observed intra-basement seismic reflector changes below the SDR, from continental crust to typical high-amplitude reflectors, probably resembling igneous rocks emplaced after the Gondwana breakup (Eldholm et al., 1995); these were accommodated along the major shear zone related to the development of the MFZ (Fig. 4) during the southward drift of the Antarctica block. This process may have facilitated the emplacement of the igneous rocks in the MB (Figs 6a and 7a).

The presence of SDR and HDLCB are commonly associated with volcanic rifted margins, (Menzies et al., 2002; Geoffroy, 2005; Mjelde et al., 2007; Franke, 2013); however, our seismic and gravity data show that the SDR is located on the interpreted basement high, bound by a major fracture zone to the east, which is characteristic of transform margins (Berndt et al., 2001; Bird, 2001). Our data indicate a thinned and intruded continental crust

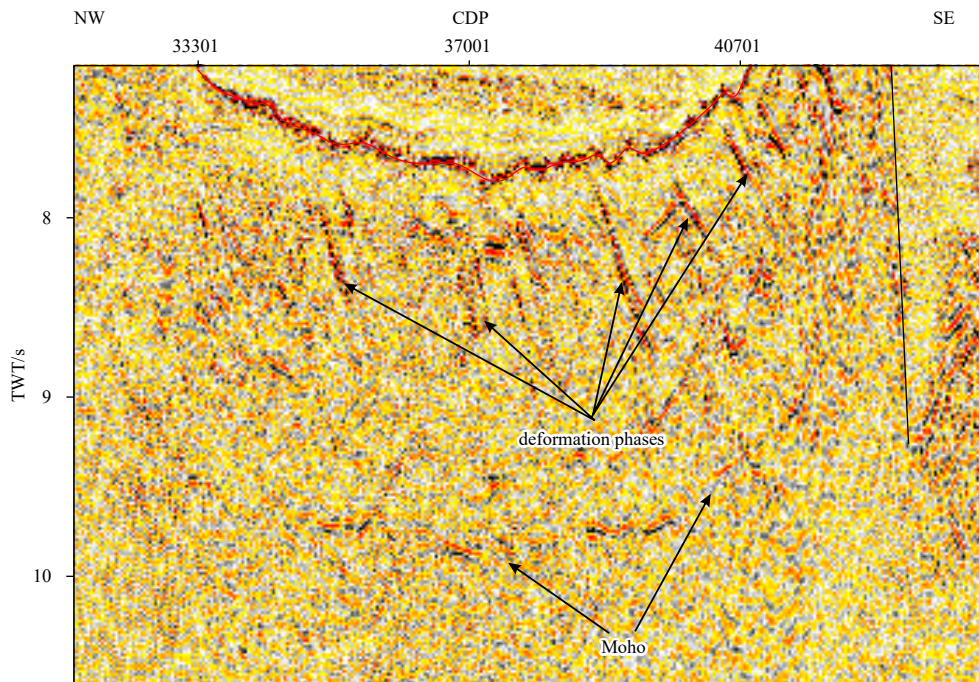


Fig. 5. Seismic profile crossing the Mozambique Basin. Shows the major fault thought to be a result of tectonic reactivation, diffractions related to deformation phases and the presence of Moho reflection at 9 s TWT. TWT: two-way travel time.

in the N-MOZR, extending and thinning seaward from the zone constrained by relatively low free-air gravity and strong negative magnetic anomalies; this continental region is about 82 km wide (Fig. 6, 50–132 km) and coincides with the location of the SDR and HDLCB that we interpreted as magmatic underplating or intrusion, as a result of rifting processes, which is in conformity with [Moulin et al. \(2019\)](#), where they did observe a high velocity layer beneath the NNV and N-MOZR based on wide-angle data.

Conversely, the thickness of the oceanic crust in the seismic01 profile is higher compared to the seismic02 profile near the N-MOZR and MB boundary. The crust in the profile seismic01 at the seaward end of the SDR wedges has ~9.5 km, about 2.4 km thicker than normal oceanic crust ((7.1 ± 0.8) km given by [White et al., 1992](#)) (Fig. 6d) and ~8.1 km for the profile seismic02 about 1 km thicker than normal oceanic crust, which is consistent with crustal thickness given by [Hanyu et al. \(2017\)](#) for the MB (Fig. 4d). In addition to the thickness of the oceanic crust, the presence of the SDR and HDLCB in the N-MOZR, demonstrates a volcanic character of the margin, and suggests that the development of the MFZ was possibly accompanied by magmatism ([Lorenzo et al., 1991](#)), implying a volcanic transform margin as the example of Vøring volcanic transform margin ([Berndt et al., 2001](#)), possibly related to the mantle–plate boundary interaction between the Antarctica block and Bouvet mantle plume ([Leinweber et al., 2011](#); [Gohl et al., 2011](#)) during the southward movement of the Antarctica block ([Leinweber and Jokat, 2012](#); [Reeves et al., 2016](#); [Klimke et al., 2018](#); [Senkans et al., 2019](#)).

East of profile seismic01 along the MB (CDP 40701–44401), we observed diffractions close to a major fault that deformed both the basement and the overlying sedimentary sequences. These diffractions are possibly related to deformation phases. We believe that the major fault is associated with tectonic reactivation that facilitated the upwelling of magmatic material, producing relatively high free-air and Bouguer gravity anomalies between 240 km and 270 km (Fig. 3) ([Ben-Avraham et al., 1995](#);

[Tikku et al., 2002](#); [Fischer et al., 2017](#)).

6.2 Implications for the demarcation of the COB

This study provides a good understanding of the COT and COB of the southern Mozambique margin. Our models reveal that it is unlikely that the N-MOZR and NNV were formed by oceanic crust, which is consistent with recent observations ([Hanyu et al., 2017](#); [Thompson, 2017](#); [Moulin et al., 2019](#)), but rather were created by thinned and intruded continental crust overlain by SDR and underlain by HDLCB.

Several studies done in the passive margins have shown that the COT is located between a clear indication of the continental crust seen through rotated fault blocks and normal oceanic crust. It is associated with abrupt changes in crustal thickness, reflecting the Moho depth changes, accompanied by changes in the associated gravity anomaly, the presence of SDR, magmatic underplating, and volcanoes ([Taylor and Hayes, 1983](#); [Menzies et al., 2002](#); [Geoffroy, 2005](#); [Franke et al., 2011, 2013](#); [Gao et al., 2015](#)). Therefore, we interpreted the abrupt changes in crustal thickness that it is evidenced by the gravity low, the shoaling of the Moho discontinuity, the presence of SDR, and the magmatic underplating or intrusion (between 50 km and 132 km) as representing the COT for the southern Mozambique margin (~82 km wide) from the stretched and intruded continental crust at the NNV (~18 km) to the thick oceanic crust (~9.5 km), separated by a shear zone which according to [Bird \(2001\)](#) is one of the characteristics of the transform margin.

The igneous complex of southeast Africa is related to three distinct periods ([Wiles et al., 2014](#)): the Early Jurassic associated with Karoo igneous activity; the Late Jurassic to Early Cretaceous associated with the breakup of Gondwana, and the period related to the southward propagation of the East African Rift System. This is consistent with well data drilled along the MCP, which identified basalts from the Early Jurassic (Fig. 1c, white circles) related to mantle plume activity prior to the breakup

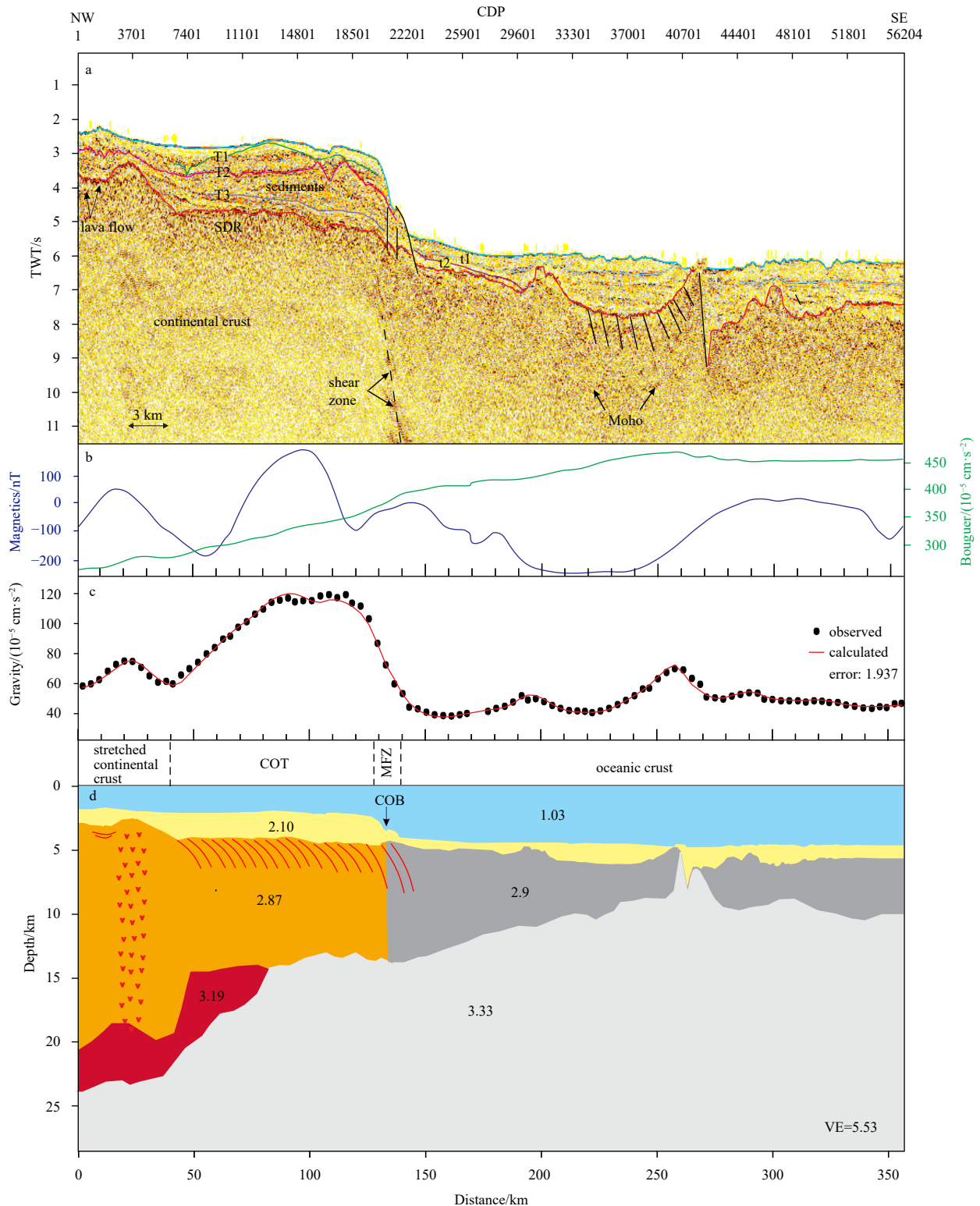


Fig. 6. Seismic interpretation of profile seismic01 across the NNV, N-MOZR, and MB (a); magnetic (blue line) and bouguer gravity (green line) anomaly profiles along the seismic01 line (b); observed and modeled free-air gravity anomaly (c); and 2D density model for profile seismic01 with density values for each block in unit of g/cm^3 (d). In a, TWT is two-way travel time; T1, T2 and T3 are stratigraphic unconformities in the N-MOZR and t1 and t2 are unconformities in the Mozambique Basin (Gao et al., 2020). For b, data are from EMAG2 (<http://geomag.org/models/emag2.html>; Maus et al., 2009) and WGM2012 (<http://bgi.omp.obs-mip.fr/data-products/Grids-and-models/wgm2012>; Bonvalot et al., 2012). In d, the solid red lines indicate the seaward dipping reflectors, the red V-shap symbol indicates the presence of an intrusion, and COB indicates continent-ocean boundary.

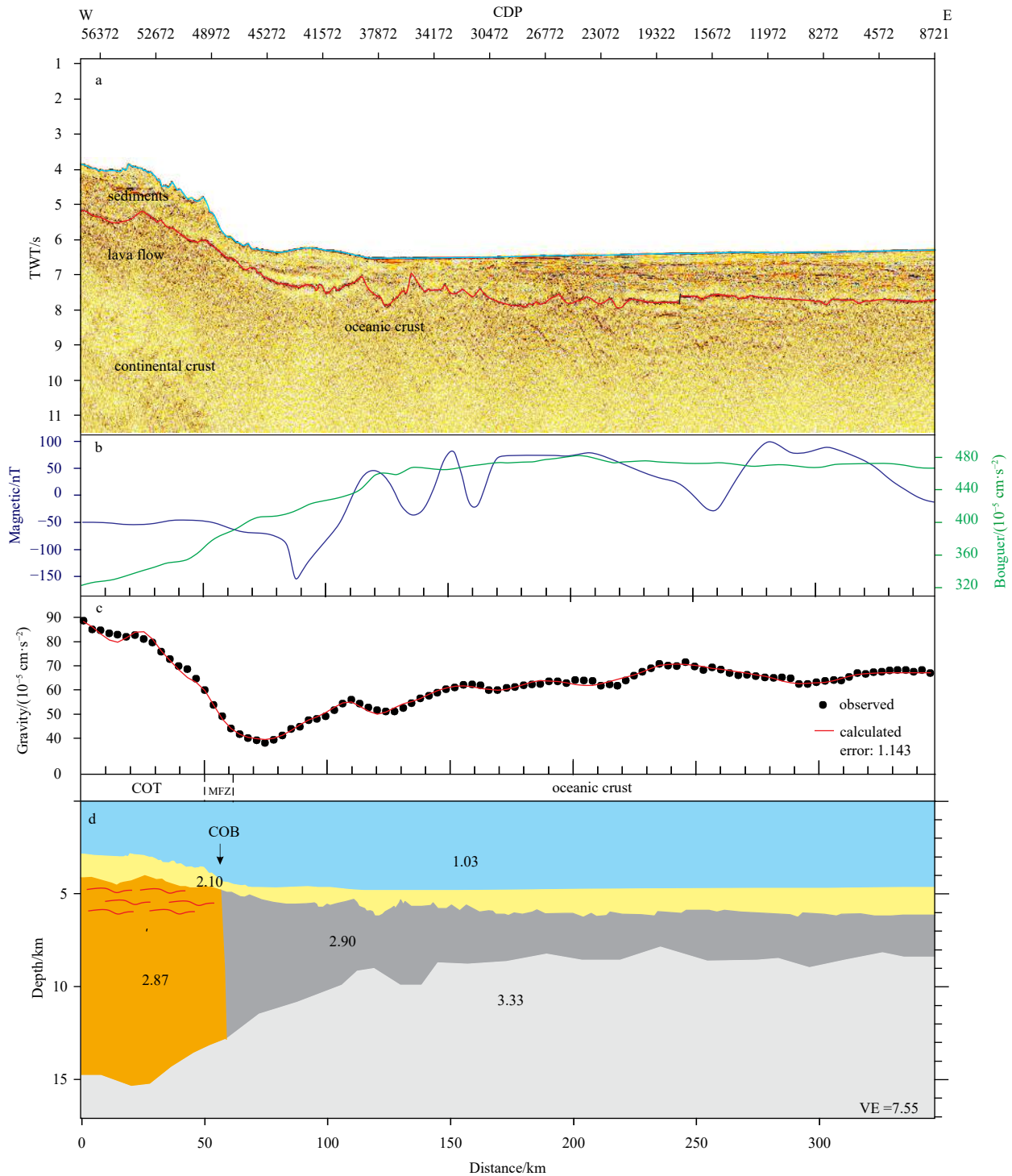


Fig. 7. Seismic interpretation of profile seismic02 at the eastern tip of N-MOZR (a); magnetic (blue line) and Bouguer gravity (green line) anomaly profiles along the seismic02 line (b); observed and modeled free-air gravity anomaly (c); and 2D density model of profile seismic02 with density values for each block in g/cm^3 (d). In a, TWT is two-way travel time. For b, data are from EMAG2 (<http://geomag.org/models/emag2.html>; Maus et al., 2009) and WGM2012 (<http://bgi.omp.obs-mip.fr/data-products/Grids-and-models/wgm2012>; Bonvalot et al., 2012). In d, the solid red lines indicate lava flow, and COB indicates continent-ocean boundary.

between Africa and Antarctica (ECL, 2000). Furthermore, three boreholes (Zandamela-1, Sunray-2, and Sunray-4) (Fig. 1c, red circles) recovered basalts from the Early Cretaceous mentioned above, also interpreted by Thompson (2017) and ECL (2000) using seismic reflection data. These basaltic intrusions were emplaced through a series of parallel fractures from west to east

(Flores, 1973; Nairn et al., 1991) as a result of lithospheric stretching in the Southern Mozambique margin (Ben-Avraham et al., 1995; Salman and Abdula, 1995; Hanyu et al., 2017), which is different from the C-MOZR and S-MOZR, known to be of oceanic origin. According to Berndt et al. (2001), the extent of the transform margin high or well known marginal ridges are usually de-

terminated by a combination of tectonic and thermal processes, which usually should have a width of 100 km or more if it was mostly controlled by tectonic processes, or less than 100 km if it was primarily controlled by thermal processes. For the N-MOZR with ~82 km wide, we believe that falls within the marginal ridges mostly controlled by thermal uplift than tectonics, which is evidenced by basaltic lava flow and magmatic underplating or intrusions in the lower crust that probably induced the thermal uplifting (Lorenzo et al., 1991). We suggest that the COB for the Southern Mozambique margin is located at the seaward termination of the SDR, where it coincides with a transition from positive to negative free-air gravity and magnetic anomalies associated with MFZ in both profiles at 132 km for the seismic01 profile (Fig. 6) and 60 km in seismic02 (Fig. 7) (Watts and Fairhead, 1999; Li and Song, 2012).

7 Conclusions

Our new 2D density models and multichannel seismic profiles across the Northern Mozambique Ridge provide an additional constraint on the crustal structure of this ridge.

The seismic data and density models reveal that the N-MOZR crust is made by thinned and intruded continental crust rather than oceanic crust. The crust underneath N-MOZR was thinned by continental extension associated with a magma-rich rifting, followed by the rupture of the MFZ during the southward drift of the Antarctica block.

The shear zone observed on multichannel seismic data suggests a transform boundary between the continental crust of the N-MOZR and the oceanic crust of the MB. We observed typical transform margin structure, such as the transform margin high, thinning seaward over a distance of ~82 km along the transition from continental to oceanic crust, and a major transform fault between the continental and oceanic crust, indicating that the evolution of the Southern Mozambique margin was also controlled by a transform margin setting.

The prominent high free-air gravity and positive magnetic anomalies represent the high-amplitude reflectors, known as seaward dipping reflectors and HDLCB, observed on the seismic profile. The presence of SDR, HDLCB, and thick oceanic crust indicates that the evolution from rifting to the development of this transform margin was accompanied by intensive magmatism, possibly as a result of the mantle–plate boundary interaction during the southward movement of Antarctica, thus suggesting a volcanic transform margin for the southern Mozambique margin.

We suggest that the N-MOZR mark the COT for the Southern Mozambique margin. Furthermore, we propose that the COB is located seaward termination of the SDR, where it coincides with a transition from positive to negative free-air gravity, magnetic anomaly, and bouguer anomaly associated with MFZ.

The Early Cretaceous basaltic intrusions at the MCP and NNV, found in data from wells Zandamela-1, Sunray-2, and Sunray-4, indicate that the lithospheric stretching in the Southern Mozambique margin was accompanied by volcanism from west to east prior to seafloor spreading. Our results are consistent with the current understanding that the COB in the Southern Mozambique margin is probably located along the MFZ.

Acknowledgements

We thank the Captain and the crew of R/V *Xiangyanghong 10* for their professional engagement and service during the China-Mozambique Joint Cruise in June 2016. We are also grateful to the State Oceanic Administration (SOA) for funding the scientific cruise. We thank Dieter Franke for the critical review of the

manuscript, and thank Dalia Lahav-Jones for editing the English text of a draft of this manuscript.

References

- Antobreh A A, Faleide J I, Tsikalas F, et al. 2009. Rift-shear architecture and tectonic development of the Ghana margin deduced from multichannel seismic reflection and potential field data. *Marine and Petroleum Geology*, 26(3): 345–368, doi: [10.1016/j.marpetgeo.2008.04.005](https://doi.org/10.1016/j.marpetgeo.2008.04.005)
- Basile C. 2015. Transform continental margins-Part 1: Concepts and models. *Tectonophysics*, 661: 1–10, doi: [10.1016/j.tecto.2015.08.034](https://doi.org/10.1016/j.tecto.2015.08.034)
- Ben-Avraham Z, Hartnady C J H, Le Roex A P. 1995. Neotectonic activity on continental fragments in the southwest Indian Ocean: Agulhas Plateau and Mozambique Ridge. *Journal of Geophysical Research: Solid Earth*, 100(B4): 6199–6211, doi: [10.1029/94JB02881](https://doi.org/10.1029/94JB02881)
- Berndt C, Mjelde R, Planke S, et al. 2001. Controls on the tectono-magmatic evolution of a volcanic transform margin: the Vøring Transform Margin, NE Atlantic. *Marine Geophysical Researches*, 22(3): 133–152, doi: [10.1023/A:1012089532282](https://doi.org/10.1023/A:1012089532282)
- Bird D. 2001. Shear margins: Continent-ocean transform and fracture zone boundaries. *The Leading Edge*, 20(2): 150–159, doi: [10.1190/1.1438894](https://doi.org/10.1190/1.1438894)
- Blaich O A, Faleide J I, Tsikalas F, et al. 2013. Crustal-scale architecture and segmentation of the South Atlantic volcanic margin. *Geological Society*, 369: 167–183, doi: [10.1144/SP369.22](https://doi.org/10.1144/SP369.22)
- Bonvalot S, Balmino G, Briais A, et al., eds. 2012. *World Gravity Map*. Paris: Commission for the Geological Map of the World. BGICGMW-CNES-IRD
- Christensen N I, Mooney W. D. 1995. Seismic velocity structure and composition of the continental crust: A global view. *Journal of Geophysical Research: Solid Earth*, 100(B7): 9761–9788, doi: [10.1029/95JB00259](https://doi.org/10.1029/95JB00259)
- Coffin M F, Rabinowitz P D. 1992. The Mesozoic east African and Madagascar conjugate continental margins: stratigraphy and tectonics. In: Watkins J S, Zhiqiang F, McMillen K J, eds. *Geology and Geophysics of Continental Margins*. Galveston, TX: The American Association of Petroleum Geologists Memoir, 53: 207–240
- Cox K G. 1992. Karoo igneous activity, and the early stages of the break-up of Gondwanaland. *Geological Society, London, Special Publications*, 68(1): 137–148, doi: [10.1144/GSL.SP.1992.068.01.09](https://doi.org/10.1144/GSL.SP.1992.068.01.09)
- Darracott B W. 1974. On the crustal structure and evolution of southeastern Africa and the adjacent Indian Ocean. *Earth and Planetary Science Letters*, 24(2): 282–290, doi: [10.1016/0012-821X\(74\)90106-X](https://doi.org/10.1016/0012-821X(74)90106-X)
- De Wit M J. 2003. Madagascar: heads it's a continent, tails it's an Island. *Annual Review of Earth and Planetary Sciences*, 31: 231–248, doi: [10.1146/annurev.Earth.31.100901.141337](https://doi.org/10.1146/annurev.Earth.31.100901.141337)
- Dingle R V, Goodlad S W, Martin A K. 1978. Bathymetry and stratigraphy of the northern natal valley (SW Indian Ocean): a preliminary account. *Marine Geology*, 28(1–2): 89–106, doi: [10.1016/0025-3227\(78\)90099-3](https://doi.org/10.1016/0025-3227(78)90099-3)
- Domingues A, Silveira G, Ferreira A M G, et al. 2016. Ambient noise tomography of the East African Rift in Mozambique. *Geophysical Journal International*, 204(3): 1565–1578, doi: [10.1093/gji/ggv538](https://doi.org/10.1093/gji/ggv538)
- Eagles G, König M. 2008. A model of plate Kinematics in Gondwana breakup. *Geophysical Journal International*, 173(2): 703–717, doi: [10.1111/j.1365-246X.2008.03753.x](https://doi.org/10.1111/j.1365-246X.2008.03753.x)
- Eagles G, Pérez-Díaz L, Scarselli N. 2015. Getting over continent ocean boundaries. *Earth-Science Reviews*, 151: 244–265, doi: [10.1016/j.earscirev.2015.10.009](https://doi.org/10.1016/j.earscirev.2015.10.009)
- Exploration Consultants Ltd (ECL), Empresa Nacional de Hidrocarbonetos (ENH). 2000. *The Petroleum Geology and Hydrocarbon Prospectivity of Mozambique '2000'*. Mozambique: Institute National Petroleum (Archives), 11: 1–144
- Eldholm O, Skogseid J, Planke S, et al. 1995. Volcanic margin con-

- cepts. In: Banda E, Talwani M, Torné M, eds. *Rifted Ocean-Continent Boundaries*, NATO ASI Series Volume. Dordrecht: Kluwer Academic Press, 1–16
- Fischer M D, Uenzelmann-Neben G, Jacques G, et al. 2017. The Mozambique Ridge: a document of massive multistage magmatism. *Geophysical Journal International*, 208(1): 449–467, doi: [10.1093/gji/ggw403](https://doi.org/10.1093/gji/ggw403)
- Flores G. 1973. The Cretaceous and Tertiary sedimentary basins of Mozambique and Zululand. In: *Sedimentary Basins of the African Coasts. Part II*. Paris: Association of African Geological Surveys
- Franke D. 2013. Rifting, lithosphere breakup and volcanism: Comparison of magma-poor and volcanic rifted margins. *Marine and Petroleum Geology*, 43: 63–87, doi: [10.1016/j.marpetgeo.2012.11.003](https://doi.org/10.1016/j.marpetgeo.2012.11.003)
- Franke D, Barckhausen U, Baristean N, et al. 2011. The continent-ocean Transition at the southeastern margin of the South China Sea. *Marine and Petroleum Geology*, 28(6): 1187–1204, doi: [10.1016/j.marpetgeo.2011.01.004](https://doi.org/10.1016/j.marpetgeo.2011.01.004)
- Gao Jinyao, Wu Siguo, McIntosh K, et al. 2015. The continent-ocean Transition at the mid-northern margin of the South China Sea. *Tectonophysics*, 654: 1–19, doi: [10.1016/j.tecto.2015.03.003](https://doi.org/10.1016/j.tecto.2015.03.003)
- Gao Ya, Stow D, Tang Yong, et al. 2020. Seismic stratigraphy and deep-water sedimentary evolution of the southern Mozambique margin: Central Terrace and Mozambique Fracture Zone. *Marine Geology*, 427: 1–18, doi: [10.1016/j.margeo.2020.106187](https://doi.org/10.1016/j.margeo.2020.106187)
- Geoffroy L. 2001. The structure of volcanic margins: some problems from the North-Atlantic/Labrador-Baffin system. *Marine and Petroleum Geology*, 18(4): 463–469, doi: [10.1016/S0264-8172\(00\)00073-8](https://doi.org/10.1016/S0264-8172(00)00073-8)
- Geoffroy L. 2005. Volcanic passive margins. *Comptes Rendus Geoscience*, 337(16): 1395–1408, doi: [10.1016/j.crte.2005.10.006](https://doi.org/10.1016/j.crte.2005.10.006)
- Gohl K, Uenzelmann-Neben G, Grobys N. 2011. Growth and dispersal of a southeast African large Igneous province. *South African Journal of Geology*, 114(3–4): 379–386, doi: [10.2113/jgssajg.114.3-4.379](https://doi.org/10.2113/jgssajg.114.3-4.379)
- Goodlad S W, Martin A K, Hartnady C J H. 1982. Mesozoic magnetic anomalies in the southern Natal Valley. *Nature*, 295(5851): 686–688, doi: [10.1038/295686a0](https://doi.org/10.1038/295686a0)
- Green A G. 1972. Seafloor spreading in the Mozambique Channel. *Nature Physical Science*, 236(63): 19–21, doi: [10.1038/physci236019a0](https://doi.org/10.1038/physci236019a0)
- Hanyu T, Nogi Y, Fujii M. 2017. Crustal formation and evolution processes in the Natal Valley and Mozambique Ridge, off South Africa. *Polar Science*, 13: 66–81, doi: [10.1016/j.polar.2017.06.002](https://doi.org/10.1016/j.polar.2017.06.002)
- Hastie W W, Watkeys M K, Aubourg C. 2014. Magma flow in dyke swarms of the Karoo LIP: Implications for the mantle plume hypothesis. *Gondwana Research*, 25(2): 736–755, doi: [10.1016/j.gr.2013.08.010](https://doi.org/10.1016/j.gr.2013.08.010)
- Hirsch K K, Scheck-Wenderoth M, Paton D A, et al. 2007. Crustal structure beneath the Orange Basin, South Africa. *South African Journal of Geology*, 110(2–3): 249–260, doi: [10.2113/jgssajg.110.2-3.249](https://doi.org/10.2113/jgssajg.110.2-3.249)
- Jacques G, Hauff F, Hoernle K, et al. 2018. Nature and origin of the Mozambique Ridge, SW Indian Ocean. *Chemical Geology*, 507: 9–22, doi: [10.1016/j.chemgeo.2018.12.027](https://doi.org/10.1016/j.chemgeo.2018.12.027)
- Jokat W, Boebel T, König M, et al. 2003. Timing and geometry of early Gondwana breakup. *Journal of Geophysical Research: Solid Earth*, 108(B9): 2428, doi: [10.1029/2002JB001802](https://doi.org/10.1029/2002JB001802)
- Klausen M B. 2009. The Lebombo monocline and associated feeder dyke swarm: Diagnostic of a successful and highly volcanic rifted margin?. *Tectonophysics*, 468(1–4): 42–62, doi: [10.1016/j.tecto.2008.10.012](https://doi.org/10.1016/j.tecto.2008.10.012)
- Klimke J, Franke D, Mahanjane E S, et al. 2018. Tie points for Gondwana reconstructions from a structural interpretation of the Mozambique Basin, East Africa and the Riiser-Larsen Sea, Antarctica. *Solid Earth*, 9(1): 25–37, doi: [10.5194/se-9-25-2018](https://doi.org/10.5194/se-9-25-2018)
- König M, Jokat W. 2010. Advanced insights into magmatism and volcanism of the Mozambique Ridge and Mozambique Basin in the view of new potential field data. *Geophysical Journal International*, 180(1): 158–180, doi: [10.1111/j.1365-246X.2009.04433.x](https://doi.org/10.1111/j.1365-246X.2009.04433.x)
- Korenaga J, Holbrook W S, Kent G M, et al. 2000. Crustal structure of the southeast Greenland margin from joint refraction and reflection seismic tomography. *Journal of Geophysical Research: Solid Earth*, 105(B9): 21591–21614, doi: [10.1029/2000JB900188](https://doi.org/10.1029/2000JB900188)
- Leinweber V T, Jokat W. 2011. Is there continental crust underneath the northern Natal Valley and the Mozambique Coastal Plains?. *Geophysical Research Letters*, 38(14): L14303, doi: [10.1029/2011GL047659](https://doi.org/10.1029/2011GL047659)
- Leinweber V T, Jokat W. 2012. The Jurassic history of the Africa-Antarctica corridor—new constraints from magnetic data on the conjugate continental margins. *Tectonophysics*, 530/531: 87–101, doi: [10.1016/j.tecto.2011.11.008](https://doi.org/10.1016/j.tecto.2011.11.008)
- Leinweber V T, Klingerhoefer F, Neben S, et al. 2013. The crustal structure of the Central Mozambique continental margin - Wide-angle seismic, gravity and magnetic study in the Mozambique Channel, Eastern Africa. *Tectonophysics*, 599: 170–196, doi: [10.1016/j.tecto.2013.04.015](https://doi.org/10.1016/j.tecto.2013.04.015)
- Li C, Song T. 2012. Magnetic recording of the cenozoic oceanic crustal accretion and evolution of the South China Sea Basin. *Chinese Science Bulletin*, 57(24): 3156–3181, doi: [10.1007/S11434-012-5063-9](https://doi.org/10.1007/S11434-012-5063-9)
- Ljones F, Kuwano A, Mjelde R, et al. 2004. Crustal transect from the North Atlantic Knipovich Ridge to the Svalbard margin West of Hornsund. *Tectonophysics*, 378: 17–41, doi: [10.1016/j.tecto.2003.10.003](https://doi.org/10.1016/j.tecto.2003.10.003)
- Lorenzo J M, Mutter J C, Larson R L. 1991. Development of the continent-ocean transform boundary of the southern Exmouth Plateau. *Geology*, 19(8): 843–846, doi: [10.1130/0091-7613\(1991\)019<0843:DOTCOT>2.3.CO;2](https://doi.org/10.1130/0091-7613(1991)019<0843:DOTCOT>2.3.CO;2)
- Lorenzo J M, Wessel P. 1997. Flexure across a continent-ocean fracture zone: the northern Falkland/Malvinas Plateau, South Atlantic. *Geo-Marine Letters*, 17(1): 110–118, doi: [10.1007/s003670050015](https://doi.org/10.1007/s003670050015)
- Lyakhovskiy V, Ben-Avraham Z, Reznikov M. 1994. Stress distribution over the Mozambique Ridge. *Tectonophysics*, 240(1–4): 21–27, doi: [10.1016/0040-1951\(94\)90261-5](https://doi.org/10.1016/0040-1951(94)90261-5)
- Müller C O. 2017. The Central Mozambique continental margin: Its tectonic evolution as the centrepiece of the initial Gondwana break-up [dissertation]. Germany: University of Bremen
- Mahanjane E S. 2012. A geotectonic history of the northern Mozambique Basin including the Beira High— A contribution for the understanding of its development. *Marine and Petroleum Geology*, 36(1): 1–12, doi: [10.1016/j.marpetgeo.2012.05.007](https://doi.org/10.1016/j.marpetgeo.2012.05.007)
- Mahanjane E S. 2014. The evolution of the East African margin offshore Mozambique: Geotectonic history and petroleum system analysis [dissertation]. Hannover: Gottfried Wilhelm Leibniz Universität Hannover. <https://d-nb.info/1058560549/04>.
- Maia M, Diamant M, Reçq M. 1990. Isostatic response of the lithosphere beneath the Mozambique Ridge (SW Indian Ocean) and geodynamic implications. *Geophysical Journal International*, 100(3): 337–348, doi: [10.1111/j.1365-246X.1990.tb00689.x](https://doi.org/10.1111/j.1365-246X.1990.tb00689.x)
- Marks K M, Tikku A A. 2001. Cretaceous reconstructions of East Antarctica, Africa and Madagascar. *Earth and Planetary Science Letters*, 186(3–4): 479–495, doi: [10.1016/S0012-821X\(01\)00262-X](https://doi.org/10.1016/S0012-821X(01)00262-X)
- Martin A K, Hartnady C J H. 1986. Plate tectonic development of the South-West Indian Ocean: a revised reconstruction of East Antarctica and Africa. *Journal of Geophysical Research: Solid Earth*, 91(B5): 4767–4786, doi: [10.1029/JB091IB05p04767](https://doi.org/10.1029/JB091IB05p04767)
- Maus S, Barckhausen U, Berkenbosch H, et al. 2009. EMAG2: A 2-arc-min resolution earth magnetic anomaly grid compiled from satellite, airborne, and marine magnetic measurements. *Geochemistry, Geophysics, Geosystems*, 10(8): 1–12, doi: [10.1029/2009GC002471](https://doi.org/10.1029/2009GC002471)
- Menzies M A, Klempnerer S L, Ebinger C J, et al. 2002. Characteristics of volcanic rifted margins. In: Menzies M A, Klempnerer S L, Ebinger C J, et al., eds. *Volcanic Rifted Margins*. Colorado: Geological Society of America, 362: 1–14
- Minshull T A. 2009. Geophysical characterisation of the ocean-continent Transition at magma-poor rifted margins. *Comptes Rendus*

- dus Geoscience, 341(5): 382–393, doi: [10.1016/j.crte.2008.09.003](https://doi.org/10.1016/j.crte.2008.09.003)
- Mjelde R, Raum T, Murai Y, et al. 2007. Continent-ocean-transitions: Review, and a new tectono-magmatic model of the Voring Plateau, NE Atlantic. *Journal of Geodynamics*, 43(3): 374–392, doi: [10.1016/j.jog.2006.09.013](https://doi.org/10.1016/j.jog.2006.09.013)
- Mjelde R, Raum T, Myhren B, et al. 2005. Continent-ocean transition on the Voring Plateau, NE Atlantic, derived from densely sampled ocean bottom seismometer data. *Journal of Geophysical Research: Solid Earth*, 110(B5): B05101, doi: [10.1029/2004JB003026](https://doi.org/10.1029/2004JB003026)
- Mougenot D, Gennesseaux M, Hernandez J, et al. 1991. La ride du Mozambique (Océan Inde): un fragment continental individualisé lors du coulisement de l'Amérique et de l'Antarctique le long de de l'Afrique de l'Est?. *Comptes Rendus de l'Académie des Sciences*, 312: 655–662
- Moulin M, Aslanian D, Evain M, et al. 2019. Gondwana breakup: messages from the North Natal Valley. *Terra Nova*, 32(3): 205–214, doi: [10.1111/TER.12448](https://doi.org/10.1111/TER.12448)
- Mueller C O, Jokat W. 2018. The initial Gondwana break-up: A synthesis based on new potential field data of the Africa-Antarctica Corridor. *Tectonophysics*, 750: 301–328, doi: [10.1016/j.tecto.2018.11.008](https://doi.org/10.1016/j.tecto.2018.11.008)
- Mueller C O, Jokat W, Schreckenberger B. 2016. The crustal structure of Beira High, central Mozambique-Combined investigation of wide-angle seismic and potential field data. *Tectonophysics*, 683: 233–254, doi: [10.1016/j.tecto.2016.06.028](https://doi.org/10.1016/j.tecto.2016.06.028)
- Nairn A E M, Lerche I, Illiffe J E. 1991. Geology, basin analysis, and hydrocarbon potential of Mozambique and the Mozambique Channel. *Earth-Science Reviews*, 30(1–2): 81–123, doi: [10.1016/0012-8252\(91\)90014-7](https://doi.org/10.1016/0012-8252(91)90014-7)
- Nguyen L C, Hall S A, Bird D E, et al. 2016. Reconstruction of the East Africa and Antarctica continental margins. *Journal of Geophysical Research: Solid Earth*, 121(6): 4156–4179, doi: [10.1002/2015JB012776](https://doi.org/10.1002/2015JB012776)
- Rabinowitz P D, Coffin M F, Falvey D. 1983. The separation of Madagascar and Africa. *Science*, 220(4592): 67–69, doi: [10.1126/science.220.4592.67](https://doi.org/10.1126/science.220.4592.67)
- Reeves C. 2014. The position of Madagascar within Gondwana and its movements during Gondwana dispersal. *Journal of African Earth Sciences*, 94: 45–57, doi: [10.1016/j.jafrearsci.2013.07.011](https://doi.org/10.1016/j.jafrearsci.2013.07.011)
- Reeves C. 2009. Re-examining the evidence from plate-tectonics for the initiation of Africa's passive margins. London: Geological Society of Houston/Petroleum Exploration Society of Great Britain, 9–10: 1–4
- Reeves C, De Wit M. 2000. Making ends meet in Gondwana: retracing the transforms of the Indian Ocean and reconnecting continental shear zones. *Terra Nova*, 12(6): 271–280
- Reeves C, Mahanjane E S. 2013. Mozambique and its role in the downfall of Gondwana. London: Geological Society of Houston/Petroleum Exploration Society of Great Britain, 11–12: 1–4
- Reeves C V, Teasdale J P, Mahanjane E S. 2016. Insight into the Eastern Margin of Africa from a new tectonic model of the Indian Ocean. *The Geological Society of London, Special Publications*, 431(1): 299–322, doi: [10.1144/SP431.12](https://doi.org/10.1144/SP431.12)
- Riley T R, Knight K. B. 2001. Age of pre-break-up Gondwana magmatism. *Antarctic Science*, 13(2): 99–110, doi: [10.1017/S0954102001000177](https://doi.org/10.1017/S0954102001000177)
- Salman G, Abdula I. 1995. Development of the Mozambique and Ruvuma sedimentary basins, offshore Mozambique. *Sedimentary Geology*, 96(1/2): 7–41, doi: [10.1016/0037-0738\(95\)00125-R](https://doi.org/10.1016/0037-0738(95)00125-R)
- Senkans A, Leroy S, D'Acremont E, et al. 2019. Polyphase rifting and break-up of the central Mozambique margin. *Marine and Petroleum Geology*, 100: 412–433, doi: [10.1016/j.marpetgeo.2018.10.035](https://doi.org/10.1016/j.marpetgeo.2018.10.035)
- Simpson E S W, Schlich R, Gieskes J M, et al. 1974. Initial Reports of the Deep Sea Drilling Project. Washington, DC, USA: US Government Printing Office, 25: 259–346
- Sutra E, Manatschal G, Mohn G, et al. 2013. Quantification and restoration of extensional deformation along the western Iberia and Newfoundland rifted margins, *Geochemistry, Geophysics, Geosystems*, 14(8): 2575–2597, doi: [10.1002/ggge.20135](https://doi.org/10.1002/ggge.20135)
- Svensen H, Corfu F, Polteau S, et al. 2012. Rapid magma emplacement in the Karoo Large Igneous Province. *Earth and Planetary Science Letters*, 325–326: 1–9, doi: [10.1016/j.epsl.2012.01.015](https://doi.org/10.1016/j.epsl.2012.01.015)
- Taylor B, Hayes D E. 1983. Origin and history of the South China Sea basin. In: Hayes D E, ed. *The Tectonic and Geologic Evolution of Southeast Asian Seas and Islands*. Washington, DC, USA: Geophysical Monograph Series: 23–56
- Thompson J O. 2017. The opening of the Indian Ocean: what is the impact on the East African, Madagascar and Antarctic margins, and what are the origins of the aseismic ridges? (in French) [dissertation]. Rennes: Université De Rennes
- Thompson J O, Moulin M, Aslanian D, et al. 2019. New starting point for the Indian Ocean: Second phase of breakup for Gondwana. *Earth-Science Reviews*, 191: 26–56, doi: [10.1016/j.earscirev.2019.01.018](https://doi.org/10.1016/j.earscirev.2019.01.018)
- Tikku A A, Marks K M, Kovacs L C. 2002. An Early Cretaceous extinct spreading center in the northern Natal Valley. *Tectonophysics*, 347(1/3): 87–108, doi: [10.1016/S0040-1951\(01\)00239-6](https://doi.org/10.1016/S0040-1951(01)00239-6)
- Voss M, Jokat W. 2007. Continent-ocean transition and voluminous magmatic underplating derived from P-wave velocity modelling of the East Greenland continental margin. *Geophysical Journal International*, 170(2): 580–604, doi: [10.1111/j.1365-246X.2007.03438](https://doi.org/10.1111/j.1365-246X.2007.03438)
- Wang Wei, Gao Jinyao, Li Dongming, et al. 2018. Measurements and accuracy evaluation of a strapdown marine gravimeter based on inertial navigation. *Sensors*, 18(3092): 1–13, doi: [10.3390/s18113902](https://doi.org/10.3390/s18113902)
- Watts A B, Fairhead J D. 1999. A process-oriented approach to modeling the gravity signature of continental margins. *The Leading Edge*, 18(2): 258–263, doi: [10.1190/1.1438270](https://doi.org/10.1190/1.1438270)
- White R S, McKenzie D, O'Nions R K. 1992. Oceanic crustal thickness from seismic measurements and rare earth element inversions. *Journal of Geophysical Research: Solid Earth*, 97(B13): 19683–19715, doi: [10.1029/92JB01749](https://doi.org/10.1029/92JB01749)
- Whitmarsh R B, Miles P R. 1995. Models of the development of the West Iberia rifted continental margin at 40°30'N deduced from surface and deep-tow magnetic anomalies. *Journal of Geophysical Research: Solid Earth*, 100(B3): 3789–3806, doi: [10.1029/94JB02877](https://doi.org/10.1029/94JB02877)
- Wiles E, Green A, Watkeys M, et al. 2014. Anomalous seafloor mounds in the northern Natal Valley, southwest Indian Ocean: Implications for the East African rift system. *Tectonophysics*, 630: 300–312, doi: [10.1016/j.tecto.2014.05.030](https://doi.org/10.1016/j.tecto.2014.05.030)